Stoichiometry Effects in GaAs Epitaxy for Ballistic Tunneling Semiconductor Devices

Jun-ichi Nishizawa and Toru Kurabayashi

Semiconductor Research Institute, Kawauchi, Aoba-ku, Sendai 980, Japan

SUMMARY: The effect of stoichiometry on various features of III-V compounds are investigated. It is shown experimentally that the optimum vapor pressure of V elements minimizes the deviation from the stoichiometric composition. Vapor pressure control technology is applied not only to the liquid phase epitaxy and bulk crystal growth but also to the surface reaction in molecular layer epitaxy.

The surface reaction and kinetic phenomena of GaAs mono-molecular layer growth by using chemical adsorption of $Ga(CH_3)_3$ (trimethyl gallium: TMG) and arsine (AsH_3) was investigated. The growth feature was strongly influenced by the surface stoichiometry of arsenic during growth. For example, the diffusion of the doped impurity is affected by the AsH_3 amount of supply, the diffusion was prevented by controlling the stoichiometry. The control of stoichiometry was examined systematically and was applied for the device fabrication such as ballistic transistor.

1. Introduction

Since in 1951, Nishizawa et al. has been studied the control of stoichiometric composition of compound [1]. From the results of annealing experiments of GaAs under controlled As vapor pressure[2], high-quality crystals have been obtained by the application of optimum As vapor pressure ($P_{GaAs,\ opt.}$). In compound semiconductor crystal, one of the most important factors to be controlled is the deviation from the stoichiometric composition. Hereafter, the stoichiometry control technology by the vapor pressure application has been extensively applied to the liquid phase epitaxial growth (LPE) [3] and the bulk crystal growth of compound semiconductor [4]. It has been shown that the nearly perfect crystals with low dislocation density were epitaxially grown under $P_{GaAs,\ opt.}$. The vapor pressure technology was successfully applied to the GaAs bulk crystal growth by the horizontal Bridegman method [5], and high quality GaAs bulk crystal have been supplied all over the world. The vapor pressure control technology was also applied to the pulling method of the GaAs bulk crystal growth, and it shown that the high-quality GaAs bulk crystals are grown with very low dislocation density below 500 cm^{-2}, which is at least two orders lower compared to those grown by the conventional liquid encapsulated Czochralski (LEC) method.

 CCC 1022-1360/98/$ 17.50

To achieve the structure of high-speed semiconductor devices, following factors are indispensable. i) precise thickness controllability with the order of atomic accuracy, ii) enough low temperature growth to avoid the incorporation of the defects and to avoid the inter diffusion from the doped layers, and iii) controllability of wide range of the doping, especially heavily doped layer is required. For these demands mono-molecular layer single crystal growth was first accomplished for these purposes in 1984 as molecular layer epitaxy (MLE) [6], which depends on the idea of atomic layer epitaxy (ALE) of II-IV compound crystals [7, 8]. MLE can produce single crystalline films monolayer by monolayer by alternate injection of component gases of the materials onto the substrate in ultra-high vacuum chamber. Until now, MLE of GaAs [9] and Si [10] have been developed with the doping methods [11]. Nishizawa et al. proposed the ideal static induction transistor (ISIT) to achieve the tera-Hertz operation [12], in which electrons transport in the crystal without collision with lattice. ISIT requires a multi-layer structure with atomic accuracy. GaAs MLE was performed to fabricate the ISIT [13], because of its thickness controllability with atomic accuracy at low temperature growth and the digital doping method which enables to the site control of the dopants. The control of the stoichiometry has also been applied for MLE in the device fabrication process.

2. Stoichiometry dependence in compound semiconductor crystals

2.1 Annealing of GaAs crystal under controlled arsenic vapor pressure

Annealing experiment on n- and p-type GaAs (100) crystals have been carried out under controlled As vapor pressure [2]. As shown in Fig. 1, a GaAs substrate and As metal were placed in a two-zone quartz ampoule, then evacuated to 3×10^{-6} Torr and sealed off. The applied arsenic pressure is controlled by the temperature of the As-zone furnace, T_{As}, independently from the heat-treatment temperature in the crystal zone, T_{GaAs}. The arsenic vapor pressure P_{GaAs} to be applied to the GaAs crystals at the temperature T_{GaAs} was determined as

$$P_{GaAs} = P_{As} \times \sqrt{T_{GaAs}/T_{As}} \qquad (1)$$

Annealing process was at 900-1100℃ for 67h; 60 um surface inhomogeneous layers were etched off before measurement. The acceptor density has a minimum value at a specific arsenic pressure ($P_{As,opt}$) which depends on the heat-treatment temperature as shown in Fig. 2. It is seen that the acceptor density is a minimum at an As pressure of about 360 Torr at

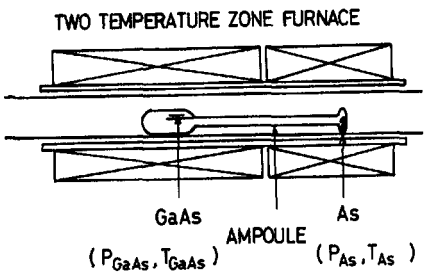

Fig. 1. Schematic of annealing experiment

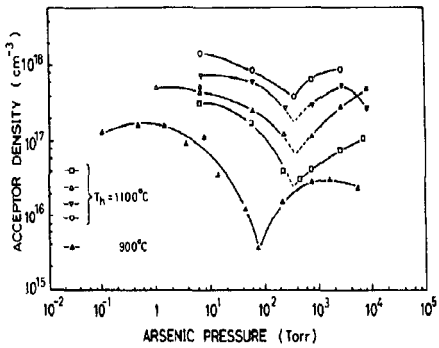

Fig. 2. Dependence of acceptor density on arsenic pressure. The acceptor density becomes a minimum at a specified arsenic pressure $P_{As,\,min}$; t_H = 67 h, Te-doped GaAs

1100 ℃ and about 80 Torr at 900 ℃. We shall denote this As pressure at which the acceptor density becomes a minimum as $P_{As,opt}$.

Arsenic pressure dependence of 1.30 eV photoluminescence and the lattice constant measured by X-ray double crystal diffractometry were measured. Also, the distinct minima can be observed, and from the equations representing the minimum point, the value of

$$P_{GaAs,opt} = 2.6\times10^{6}\exp[-1.05(eV)/(kT)]\ \text{Torr}, \qquad (2)$$

can be obtained.

The photocapacitance (PHCAP) method was applied to determine the deep level energy and the density of Au in Si with the irradiation of monochromatic light by Nishizawa [14]. The junction capacitance was kept constant by the control of the bias voltage according to the change of ion density in the depletion region in the constant capacitance method. Precise description of the PHCAP method and the apparatus is shown in the other paper [15]. In Fig. 3, trace (a) shows the PHCAP spectrum of the undoped HB GaAs crystals annealed under excess of As pressure of 4.66×10^{2} Pa. This As pressure is extremely low compared to the optimum vapor pressure of As. The PHCAP responses due to two kinds of deep donors at Ec-0.66 and 0.72 eV and the photoquenching level decreased drastically compared to the not-annealed sample. Trace (b) also shows the PHCAP spectrum of undoped HB GaAs crystals annealed under excess of arsenic vapor pressure at 2.6×10^{5} Pa which is much higher than $P_{As,opt}$ at 900 ℃ for 67h. In this plot, the Ec-0.72 eV deep donor can be detected clearly and the Ec-0.66 eV deep donor will be annihilated. For comparison, trace (c) shows the PHCAP spectrum of undoped HB GaAs before annealing. The Ec-0.66

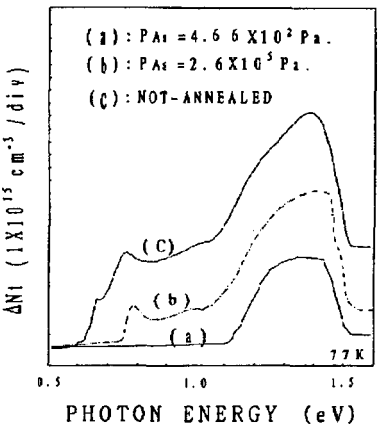

Fig. 3. Arsenic vapor pressure dependence of the maximum ion density PHCAP spectrum. Annealing was carried out at 900 °C for 67 h under various arsenic pressure

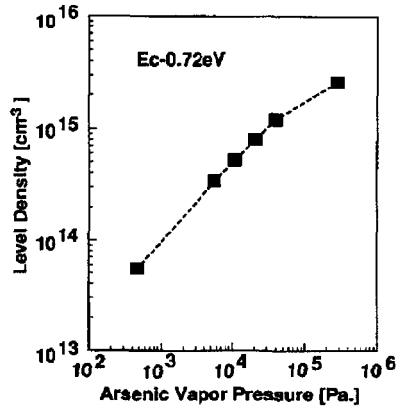

Fig. 4. Arsenic vapor pressure dependence of Ec-0.72 eV level density in the intentionally-undoped HB GaAs. Annealing was carried out at 900 °C for 67 h under various arsenic pressure

eV deep donor vanishes or drastically decreases in density after annealing because of its thermal instability. Fig. 4 shows the relationship between the applied arsenic vapor pressure and the Ec-0.72 eV deep donor density as obtained by the PHCAP measurement. It was shown that the Ec-0.72 eV level density increased with increasing of As vapor pressure during annealing. From these results it is concluded that the Ec-0.72 eV deep donor is attributable to the excess As composition in GaAs. Many properties of these specimens have been studied including: specific weight, anormalous X-ray transmission, photo-luminescence Rutherford back-scattering etc.

At this time the non-stoichiometry was interpreted in terms of Ga vacancies and interstitials. However, we introduced the idea of As interstitials and vacancies. Recently, the idea of anti-site As has emarged as the most popular idea to explain non-stoichiometry effects. However, at least at the beginning of non-stoichiometry, the As interstitial should be formed at the crystal surface. Direct generation of anti-site defect seems to be difficult to explain.

2.2 Liquid phase epitaxial growth of GaAs by the temperature difference method under controlled vapor pressure (TDM-CVP)

If we establish a slight temperature difference in the liquid phase epitaxy (LPE) crucible and place a substrate in the lower temperature region, the difference of the saturation

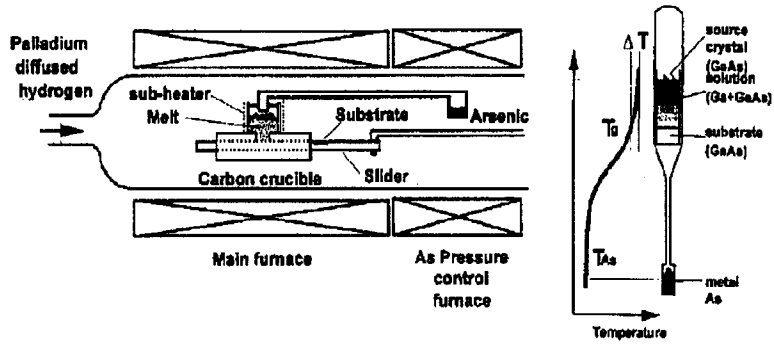

Fig. 5. Schematic drawing of the LPE equipment by the temperature difference method under controlled vapor pressure (TDM-CVP)

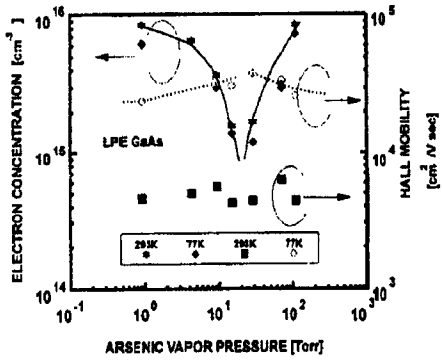

Fig. 6. As vapor pressure dependences of the electron density and the Hall mobility of LPE-grown GaAs by the TDM-CVP. Epitaxial growth was carried out at constant substrate temperature of 700 °C in the Pd-diffused hydrogen atmosphere

solubility and in the kinetic energy induces two sorts of diffusion toward the lower temperature region, followed by the segregation of the solute materials. At the same time, if the source materials are placed in the higher temperature region, continuous transport of the materials takes place during growth of epitaxial crystal on the substrate. This method is temperature difference method (TDM) in LPE [3]. In addition, the vapor pressure technology for the stoichiometry control as in the case of the heat-treatment has been applied successfully as TDM-CVP. Fig. 5 shows the schematic drawing of the LPE equipment. The epitaxial growth proceeds at a constant substrate temperature.In order to control the stoichiometry of the segregated crystals, the vapor pressure of the group V element is applied onto the solution. The epitaxial growth was carried out in the Pd-diffused hydrogen.

Fig. 6 shows the As vapor pressure dependence of the electron density and the Hall

mobility. It is shown that the high-purity GaAs is epitaxially grown under specific As vapor pressure. In addition, from the crystallographic characteristics, the lattice constant and the FWHM value of the X-ray rocking curve measured by the X-ray double crystal diffractometry show its minimum value under the same As vapor pressure region.

3. Effects of the stoichiometry on the surface reaction in MLE GaAs

3.1 Effect of surface stoichiometry on MLE reaction

Fig. 7 shows the schematic diagram of MLE system and gas injection sequence. The growth chamber was evacuated by a turbo-molecular pump and rotary pump. The net pumping speed was about 200 l/s, and the background pressure was about 1×10^{-9} Torr. The arsenic source was pure AsH_3 (100%), and the gallium source was pure TMG or $Ga(C_2H_5)_3$ (triethylgallium: TEG) without carrier gas.

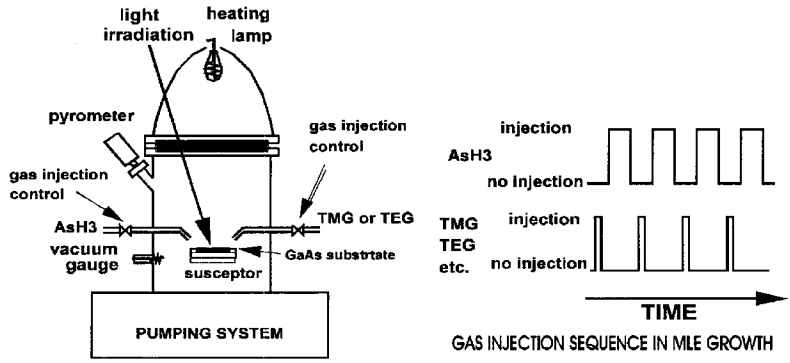

Fig. 7. Schematic diagram of MLE system and gas injection sequence

Temperature dependence

Fig. 8 shows the dependence of the growth rate per cycle on the growth temperature in TMG- AsH_3 [16]. The growth sequence was 100"-4"-16"-4"; a 100s AsH_3 injection, a 4 s evacuation of AsH_3, a 16 s TMG injection, and a 4 s TMG evacuation. The injected TMG pressure was constant at 5×10^{-5} Torr, and AsH3 pressure was 1×10^{-3} Torr. Monolayer growth occurred at the temperatures from 445 to 522 °C and the smooth surface morphology was observed. When the injection pressure of TMG was changed the temperature region of the plateau was also changed. Higher pressure and shorter duration of TMG supply showed wider plateau.

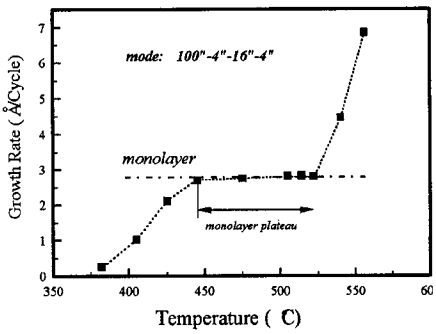

Fig. 8. Growth rate dependence on growth temperature in MLE

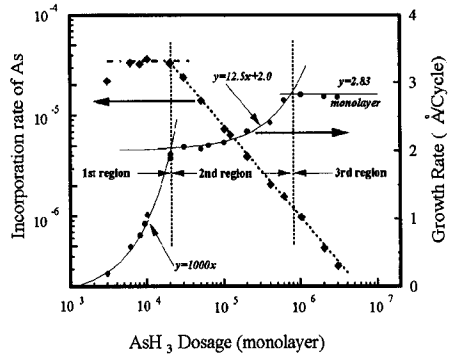

Fig. 9. Growth rate per cycle as a function of AsH_3 dosage in MLE

AsH_3 supply

Fig. 9 shows the growth rate per cycle at 513 °C versus AsH_3 dosage, which means the product of the pressure and the duration of AsH_3 in each cycle [16]. In the figure, there were three different characteristics of the growth rate versus AsH_3 dosage. The growth rate per cycle in molecular layer epitaxy by using TMG and AsH_3 was strongly influenced by the surface stoichiometry of arsenic on the growing surface. The dominant parameter was the product of the AsH_3 pressure and its duration. There are two stable state of arsenic at near 70% of arsenic coverage and 100% arsenic coverage, respectively. One is near 70% coverage which is found at a lower AsH_3 dosage and the other is almost 100% coverage at the excess AsH_3 dosage. Chadi predicted two different structures of (2×4) As-stabilized surface [17]. One is (2×4)γ with an arsenic coverage of 100% (monolayer), and the other is (2×4)β with an As coverage of 75% (3/4 monolayer). The coverage of 75% may fit our result of 2 Å state (70% coverage of arsenic).

TMG supply

Fig. 10 shows the growth rate and the incorporation rate of Ga versus TMG pressure. The growth mode was 100"-4"-16"-4", and the pressure of TMG was changed. The incorporation rate means the probability of Ga incorporated into the lattice of the GaAs from a molecule of TMG in a cycle. When the TMG pressure was from 1.5×10^{-6} to 5.0×10^{-6} Torr, the growth rate per cycle exceeded monolayer height, and the surface was rough (enhanced growth). Whereas the TMG pressure was over 1×10^{-5} Torr, monolayer growth occurred and mirror-like surface was obtained. The incorporation rate of Ga from TMG was nearly constant at the TMG pressure under 2×10^{-6} Torr, and decreased gradually with increasing TMG pressure in the range over the value. Thus, the Ga or Ga compound on the

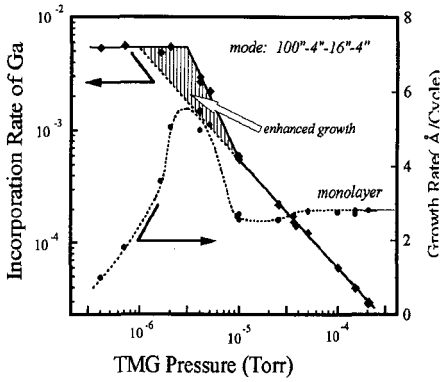

Fig. 10. Growth rate per cycle as a function of TMG pressure in MLE

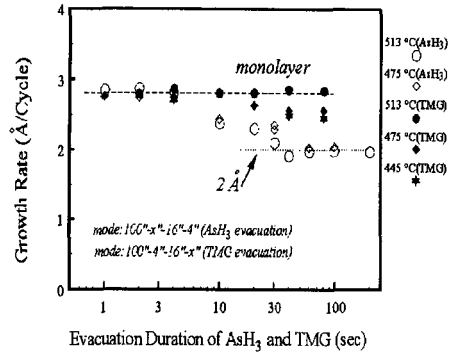

Fig. 11. The dependence of the growth rate per cycle on the evacuation duration of AsH_3 and TMG

surface may not interact with TMG at pressures under 2×10^{-6} Torr, while the interaction rate may increases gradually with increasing TMG pressure.

Evacuation of AsH_3 and TMG

The dependence of the growth rate per cycle on the evacuation duration of AsH_3 and TMG was investigated (11) as shown in Fig. 11 [16]. On the monolayer growth condition, AsH_3 was introduced for 100 s at the pressure of 1×10^{-3} Torr and TMG for 16 s at 5×10^{-5} Torr. In the figure, ○ and ◇ indicate the dependence on AsH_3 evacuation duration. Almost complete monolayer growth occurred when the evacuation duration of AsH_3 was shorter than 4 s, but the growth rate per cycle decreased gradually with increasing the evacuation duration of AsH_3 and saturated near 2 Å which coincides with the 70% coverage saturation of arsenic as discussed. It is suggested that the arsenic coverage changes from 100% to 70% by increasing the duration of AsH_3 evacuation. The arsenic re-evaporate from the arsenic monolayer covered surface.

The dependence of growth rate per cycle on the TMG evacuation duration is shown in Fig. 11 as a function of growth temperature. In the case of the temperature at 513 °C (●), the growth rate per cycle was always the value of a monolayer. On the other hand, the growth rate per cycle decreased with increasing evacuation duration of TMG and probably saturated over 40 s at the temperatures of 475 and 445 °C. The adsorbate formed by TMG supply might not be Ga but Ga compounds which would be volatile and re-evaporate during the TMG evacuation in the case of 475 and 445 °C.

3.2 Surface reaction mechanism in MLE

The reaction products from the surface reaction during MLE were measured by in-situ

mass spectroscopy [18]. It appears that at least two reactions occur during TMG injection. One is the initial state reaction corresponding to the rapid increase of amu 15 CH_3^+ and the rapid decrease of amu 99 $Ga(CH_3)_2^+$. The other is the steady state reaction which corresponds to the formation of amu 84 $GaCH_3^+$ as the dominant species. At 420-510 °C the monolayer of $GaCH_3$ would be formed by the introduction of TMG temporarily, from which adsorbed Ga and desorbed CH_3 with a time constant of 15-36 s are formed. The time constant of formation of the Ga adsorbed layer is longer if the substrate temperature is lower. The further decomposition of TMG occurs on this Ga adsorbed layer. The products of this reaction might be such volatile molecules as $GaCH_3$ or $Ga(CH_3)_2$. The reaction of TMG on GaAs (100) are as follows.

$$Ga(CH_3)_3 \text{ -----> } GaCH_3 \text{ (ad) } +2\ CH_3 \text{ (initial state), (3)}$$

$$GaCH_3 \text{ (ad) -----> } Ga \text{ (ad) } + CH_3 \text{ (transient state), (4)}$$

$$Ga(CH_3)_3 \text{ -----> } GaCH_3 + 2CH_3 \qquad \text{or}$$

$$Ga(CH_3)_3 \text{ -----> } Ga(CH_3)_2 + CH_3 \text{ (steady state). (5)}$$

The reaction between AsH_3 and the adsorbed species associated with the TMG injection was also measured by QMS. As a result, an amu 2 H_2^+ signal along with a weaker amu 15 CH_3^+ signal was observed. This means that CH_4 and H_2 are the byproducts of the reaction with a long time constant (>30 s). We concluded that the main adsorption species formed by the TMG injection would be $GaCH_3$. From the QMS data, the possible reactions with AsH_3 are

$$GaCH_3(\text{adsorb}) + AsH_3 \text{ -----> } GaAs + CH_4 + H_2, \qquad (6)$$

The reaction in MLE was schematically shown in Fig. 12.

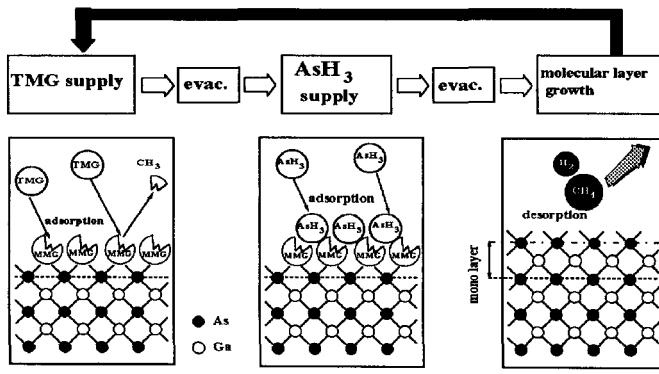

Fig. 12. Schematical draw of the surface reaction mechanism of TMG and AsH_3 in MLE

3.3 Effect of surface stoichiometry on the re-grown interface for ISIT

Nishizawa et al. proposed the ideal static induction transistor (ISIT) to achieve the tera-Hertz operation [19], in which electrons transport in the crystal without collision with lattice. ISIT requires a multi-layer structure with atomic accuracy. GaAs MLE was performed to fabricate the ISIT [20]. As shown in Fig. 13, electrical source-drain distance of 170 Å was achieved, i.e. the ballistic, collision-less transport of electrons is expected, since the drain-source distance is shorter than the mean free path of the electrons in GaAs crystal, which is nearly 1000 Å. The static induction transistor (SIT) has vertical structure and was fabricated with two MLE processes. The thin p^{++} layer introduced between the drain and the source induces a potential barrier Ψb preventing the drain-source shorting far away from the active edge. The regrown channel-gate structure consists of a grown first, few monolayer thick n^{++} layer, then an unintentionally doped u layer, the p^{+} gate and finally the p^{++} contact cap. The thin n^{++} layer at the regrown interface is introduced to create a potential barrier minimum, i.e. a saddle, so that the stream of injected electron flowing down from the source to the drain can confined near the regrown interface. In this device, electron transport between the source and the drain can be collisionless and ballistic. As shown in Fig. 13 electrons which have higher energy than the barrier are thermionically injected from the source to the drain. However, electrons of lower energy at the source are reflected by the potential barrier and scattered consequently. When the distances of source-drain are on the order of 100 Å a significant tunneling of carriers should also be considered.

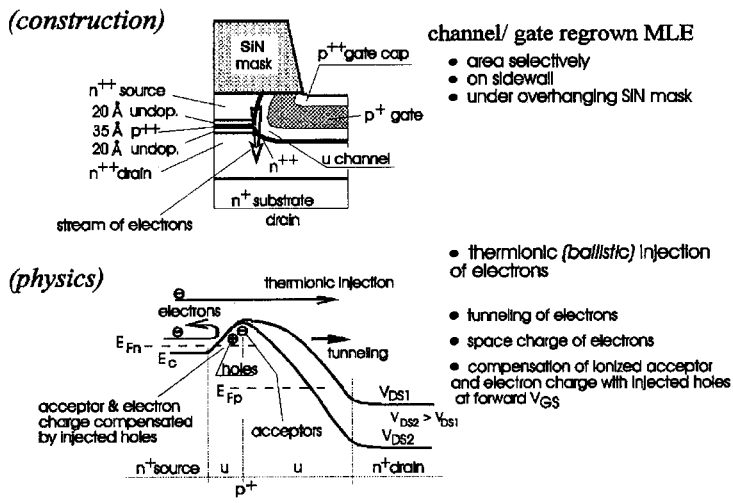

Fig. 13. 170 Å (80 Å) GaAs ideal static induction transistor

In the fabrication process of ISIT, the first epitaxial process is the source-drain fabrication, and the second is the regrowth gate fabrication. Prior to the regrowth, the surface treatment by heating was necessary to remove the surface contaminations. Figure 14-1 shows the current-voltage (I-V) characteristics of the regrown GaAs *pin* diode on Si doped ($n=2\times10^{18}$ cm-3) GaAs (100), which corresponds to the gate structure of ISIT [21]. MLE growth temperature was fixed to be 420 °C. In the figure, "high_temp" means that the surface treatment was done at 620 °C under the AsH_3 pressure of 2×10^{-4} Torr for 30 min. The "opt" means the optimized surface treatment condition i.e. under the AsH_3 pressure of 8×10^{-4} Torr at 480 °C for 30 min. The "high_press" is the surface treatment condition under the AsH_3 pressure of 1×10^{-3} Torr at 480 °C for 30 min. "no_AsH_3" indicates the condition without AsH_3 at 480 °C for 30 min. The I-V characteristics of "contin" was obtained by the continuously grown (not regrown) pin diode. In view of defect in the depletion layer with regrown interface, the current at a specific forward voltage (Vf*) reflects the density of recombination centers. Figure 14-2 shows the treatment temperature dependence of Vf*. The AsH_3 pressure was kept constant at 2×10^{-4} Torr and the treatment time was 30 min. Vf* shows it maximum value at 510 °C and that the high temperature treatment seems to degrade the regrown interface. Furthermore, the change of Vf* as a function of AsH_3 pressure during surface treatment was examined. At 480 °C, Vf* shows the maximum value at the AsH_3 pressure of 8×10^{-4} Torr. It should be noticed that the maximum value of Vf* at 510 °C is lower than that at 480 °C at the surface treatment time of 30 min., as shown in the other paper [21].

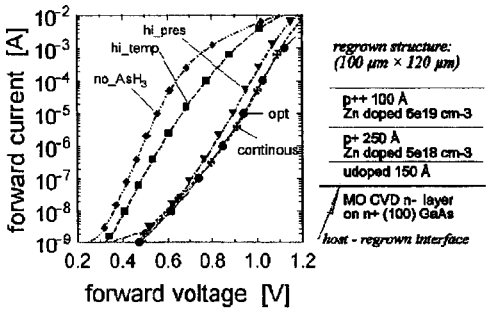

Fig. 14-1. Current voltage characteristics of the regrown GaAs pin diodes prepared by MLE

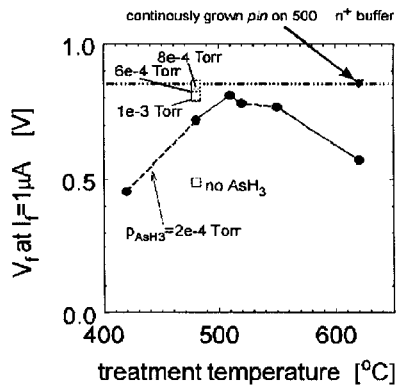

Fig. 14-2. Temperature treatment dependence of specific forward bias voltage of regrown GaAs pin diodes

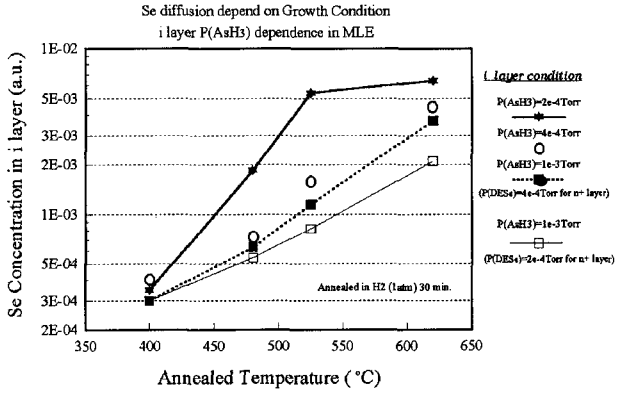

Fig. 15-1. Diffused Se concentration in i layer vs. annealed temperature. The structure was n^+ (Se doped 500 Å)-i (undoped 500 Å) on semi-insulating GaAs(100). The growth condition of i layer was changed as a parameter of AsH_3 injection pressure

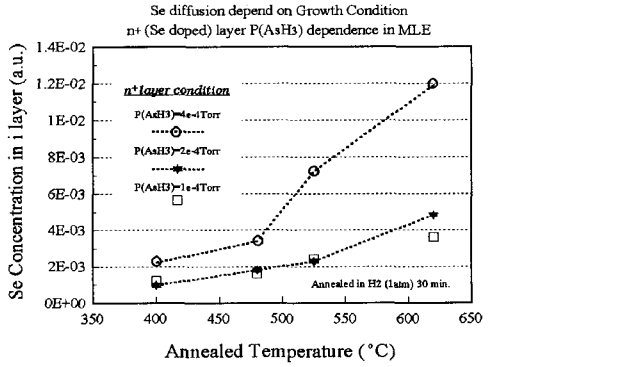

Fig. 15-2. Diffused Se concentration in i layer vs. annealed temperature. The structure was n^+(Se doped 500 Å)-i (undoped 500 Å) on semi-insulating GaAs(100). The growth condition of n^+ layer was changed as a parameter of AsH_3 injection pressure

3.4 Effect of surface stoichiometry on the impurity doping

Doping MLE was applied using TEG and AsH_3 to grow GaAs films by changing the substrate temperature during the growth cycle according to the source gas injection(12). The source gas injection was synchronized with the substrate temperature, in a growth cycle of undoped temperature synchronized-MLE [22]. The effect of the doping period was studied by the following experiments in which the dopant source was supplied at AsH_3 evacuation period (AA), at TEG injection period (IG) , at TEG evacuation period (AG) ,or at AsH_3 injection period (IA)(8). The hole concentration of the Zn doped films was controllable in the range of 4×10^{18} cm^{-3} to 1×10^{20} cm^{-3}, and the electron concentration of the Se doped films was in the range of 4×10^{18} cm^{-3} to 5×10^{19} cm^{-3}. These doping levels

of p type and n type are also influenced by the stoichiometry in growth condition i.e. AsH_3 pressure and/or injection duration. To examine the stoichiometry dependence of growth condition on impurity diffusion, n^{++} (Se doped 500 Å)-i (undoped 500 Å) structure was fabricated by doping MLE in various condition of AsH_3 supply. These samples were heat-treated after growth at temperatures of 480, 525 and 620 °C for 30 min in H_2 atmosphere. The diffused Se concentrations in i layer versus annealed temperature were plotted as parameters of AsH_3 injection pressure in i layer growth and in n^{++} layer growth in Fig. 15-1 and -2, respectively. The growth condition for i layer to prevent the Se diffusion requires large amount of AsH_3 supply. However, the condition for n^{++} layer to prevent the Se diffusion requires low pressure AsH_3 supply i.e. small amount of AsH_3 supply. In the case of i layer condition, arsenic-rich crystal has a lack of As vacancy and prevent the diffusion of Se which may be located in As site preferentially as a donor. On the contrary, in n^{++} layer, As vacancy which is formed under the condition of small amount of AsH_3 supply may act as a getter of diffused Se. These monolayer crystal growth technologies under controlled surface stoichiometry during growth will realize the sub-monolayer devices which have a steep distribution of impurities.

4. Conclusive remarks

It has been shown that the deviation from the stoichiometric composition governs almost all the characteristic features of compound semiconductor materials. The control of stoichiometry is one of the most important factors not only for bulk or LPE grown layer but also for the surface science. It is also shown that the surface reaction in MLE is affected by the surface stoichiometry.

Urgent requirement for recent and future semiconductor devices is more fine structure for improved device performances. As in the case of ideal static induction transistor (ISIT), electron cannot sense collisions with crystal lattices and transport with their thermal energy through gate potential region. These kinds of devices can never be achieved without precise controllability of the epitaxial process with atomic accuracy. The detail understandings of the semiconductor process mechanisms and the control of the surface phenomena with stoichiometry control during process enable the successful achievement of the multi-thin layered structure devices.

References

1. Y. Watanabe, J. Nishizawa, and I. Sunagawa, Kagaku 21, Iwanami (1951) 140
2. H. Otsuka, K. Ishida, and J. Nishizawa, Jpn. J. Appl. Phys.. 8, (1969) 632,

   J. Nishizawa, H. Otsuka, S. Yamakoshi and K. Ishida, Jpn. J. Appl. Phys., 13 (1974) 46
3. J. Nishizawa, H. Tadano and Y. Okuno, J. Cryst. Growth. 31, (1975) 215
4. K. Tomizawa, K. Saaas, Y. Shimanuki and J. Nishizawa, J. Electrochem. Soc 131, (1984) 2394
5. T. Suzuki, S. Akai, Bussei 144, (1971) 12
6. J. Nishizawa, and Y. Kokubun; Extended Abstract of 16th International Conference on Solid State Devices and Materials, 1984, p1.
7. T. Suntola; U.S. Pat. No. 4058430 (1977).
8. M. Ahonen, M. Pessa, and T. Suntola; Thin Solid Films 65 (1980) 301.
9. J. Nishizawa, H. Abe, and T. Kurabayashi; J. Electrochem. Soc. 132 (1985) 1197
10. .J. Nishizawa, K. Aoki, S. Suzuki, and K. Kikuchi; J. Electrochem. Soc. 137 (1990) 1898.
11. J. Nishizawa, H. Abe, T. Kurabayashi; J. Electrochem. Soc. 136 (1989) 478.
12. J. Nishizawa, T. Terasaki and J. Shibata; IEEE Trans. Electron. Devices ED-22 (1975) 185.
13. P. Plotka, T. Kurabayashi, Y. Oyama and J. Nishizawa; Applied Surface Science 82/83 (1994) 91.
14. A. Itoh, T. Sukegawa and J. Nishizawa, Tech. Report of Transistor Specialist Committee, IEE Japan (Jan 1967)
15. J. Nishizawa, Y. Oyama and K. Dezaki, J. Appl. Phys., 67 (1990) 1884
16. J. Nishizawa and T. Kurabayashi; J. Vac. Sci. Technol. B13(3) (1995) 1024
17. D. J. Chadi; J. Vac. Sci. Technol. A 5 (1987) 834
18. J. Nishizawa, H. Sakuraba and T. Kurabayashi; J. Vac. Sci. Technol. B14(1) (1996) 136
19. J. Nishizawa, T. Terasaki and J. Shibata, IEEE Trans. Electron Devices, ED-22(4) (1975) 185
20. P. Plotka, T. Kurabayashi, Y. Oyama and J. Nishizawa, Applied Surface Science 82/83, (1994) 91
21. Y. Oyama, P. Plotka and J. Nishizawa, Applied Surface Science 82/83, (1994) 41
22. T. Kurabayashi and J. Nishizawa, Applied Surface Science 82/83, (1994) 97